



Published in final edited form as:

Genes Chromosomes Cancer. 2011 June ; 50(6): 466–477. doi:10.1002/gcc.20872.

Identification of Intragenic Deletions and Duplication in the *FLCN* Gene in Birt-Hogg-Dubé Syndrome

Jihane N. Benhammou¹, Cathy D. Vocke¹, Avni Santani², Laura S. Schmidt^{1,3,*}, Masaya Baba¹, Kuniaki Seyama⁴, Xiaolin Wu⁵, Susana Korolevich⁵, Katherine L. Nathanson⁶, Catherine A. Stolle², and W. Marston Linehan¹

¹ Urologic Oncology Branch, NCI, NIH, Bethesda, MD, 20892 USA

² Molecular Genetics Laboratory, Department of Pathology and Laboratory Medicine, Children's Hospital of Philadelphia, Abramson Research Center, Philadelphia, PA USA

³ Basic Science Program, SAIC-Frederick, Inc., NCI-Frederick, Frederick, MD 21702 USA

⁴ Department of Respiratory Medicine, Juntendo University School of Medicine, Tokyo, Japan

⁵ Laboratory of Molecular Technology, SAIC-Frederick, Inc., NCI-Frederick, Frederick, MD 21702 USA

⁶ Abramson Cancer Center at the University of Pennsylvania and Department of Medicine, Division of Medical Genetics, University of Pennsylvania, Philadelphia, PA USA

Abstract

Birt-Hogg-Dubé syndrome (BHDS), caused by germline mutations in the *folliculin* (*FLCN*) gene, predisposes individuals to develop fibrofolliculomas, pulmonary cysts, spontaneous pneumothoraces and kidney cancer. The *FLCN* mutation detection rate by bidirectional DNA sequencing in the National Cancer Institute BHDS cohort was 88%. To determine if germline *FLCN* intragenic deletions/duplications were responsible for BHDS in families lacking *FLCN* sequence alterations, 23 individuals from 15 unrelated families with clinically-confirmed BHDS but no sequence variations were analyzed by real-time quantitative PCR (RQ-PCR) using primers for all 14 exons. Multiplex Ligation-Dependent Probe Amplification (MLPA) Assay and array-based comparative genomic hybridization (CGH) were utilized to confirm and fine map the rearrangements. Long Range PCR followed by DNA sequencing was used to define the breakpoints. We identified 6 unique intragenic deletions in 9 patients from 6 different BHDS families including four involving exon 1, one that spanned exons 2–5, and one that encompassed exons 7–14 of *FLCN*. Four of the six deletion breakpoints were mapped, revealing deletions ranging from 5688 to 9189bp. In addition, one 1341bp duplication, which included exons 10 and 11, was identified and mapped. This report confirms that large intragenic *FLCN* deletions can cause BHDS and documents the first large intragenic *FLCN* duplication in a BHDS patient.

*Correspondence: Laura S. Schmidt, Ph.D., National Cancer Institute, Bldg 10/CRC/1-3961, 10 Center Drive MSC1107, Bethesda, MD 20892, schmidtl@mail.nih.gov, Phone: 1-301-402-4707, Fax: 1-301-480-3195.

COMPETING INTERESTS

None.

WEB RESOURCES

The URLs for data presented are as follows:

National Center for Biotechnology Information BLAST program:

<http://www.ncbi.nlm.nih.gov/BLAST/>

Detection of *Alu* repeat sequences with RepeatMasker: <http://www.repeatmasker.org>

UCSC human genome browser: <http://genome.ucsc.edu/>

Proscan Version 1.7: <http://www.bimas.cit.nih.gov/>

Additionally, we identified a deletion “hot spot” in the 5′-noncoding-exon 1 region that contains the putative *FLCN* promoter based on a luciferase reporter assay. RQ-PCR, MLPA and aCGH may be used for clinical molecular diagnosis of BHDS in patients who are *FLCN* mutation-negative by DNA sequencing.

Keywords

Birt-Hogg-Dubé syndrome; *FLCN* deletion/duplication mutation; BHD; RQ-PCR; MLPA

INTRODUCTION

Birt-Hogg-Dubé Syndrome (BHDS;MIM135150) is an autosomal dominant disorder that predisposes individuals to develop fibrofolliculomas, pulmonary cysts, pneumothoraces and kidney neoplasia(Birt et al., 1977; Toro et al., 1999). The BHDS locus was mapped to chromosome 17p11.2 (Schmidt et al., 2001) and germline mutations in a novel gene, *FLCN*, (MIM607273) were identified in affected members of BHDS families (Nickerson et al., 2002). The 14 exon gene encodes folliculin (FLCN), a novel protein that is highly conserved across species. The identification of somatic “second hit” *FLCN* mutations in the remaining wild-type allele in BHD-associated renal tumors suggests a tumor suppressor role, consistent with the Knudson “two-hit” hypothesis (Vocke et al., 2005). Additionally, *FLCN* mRNA levels were reduced in renal tumors from BHDS patients (Warren et al., 2004) and FLCN protein could not be detected in BHD renal tumors or *Fln* heterozygous knockout mice (Hasumi et al., 2009).

A spectrum of germline *FLCN* mutations in patients with BHDS has been reported, including small insertion/deletions, splice-site, and nonsense mutations predicted to prematurely truncate the protein and, rarely, missense mutations (Toro et al., 2008; Schmidt et al., 2005). To date, 88% of 102 clinically-proven BHDS families in the NCI cohort have sequence-identified *FLCN* mutations (Toro et al., 2008).

Large intragenic rearrangements have been reported in the cancer predisposing genes *von Hippel-Lindau* (*VHL*[MIM608537]) (Franke et al., 2009; Hoebeeck et al., 2005; Hattori et al., 2006), *succinate dehydrogenase subunit B* (*SDHB*[MIM185470]) (McWhinney et al., 2004), *fumarate hydratase* (*FH*[MIM136850]) (Ahvenainen et al., 2008) and *breast cancer 1* (*BRCA1*[MIM113705]) (Swensen et al., 1997). Recently Kunogi et al. (Kunogi et al., 2010) published the first report of large intragenic *FLCN* deletions in two unrelated BHDS patients. We speculated that large intragenic deletions and/or duplications in the *FLCN* gene might account for some of the 12% of families in the NIH BHDS cohort for whom *FLCN* sequence variants have not been identified.

PATIENTS AND METHODS

Patients and DNA samples

Patients with clinically-confirmed Birt-Hogg-Dubé syndrome that were negative for a mutation by bidirectional DNA sequencing of the 14 *FLCN* exons were selected for this study. Most patients were seen at the Urologic Oncology Branch, National Cancer Institute, National Institutes of Health for clinical assessment and provided a peripheral blood sample for DNA extraction. Additional family members were evaluated during field trips. This study was approved by the Institutional Review Board of the National Cancer Institute. All patients provided written informed consent.

Real-Time Quantitative PCR (RQ-PCR)

RQ-PCR was conducted on an ABI Prism 7000 Sequence Detection System (Applied Biosystems) using SYBR Green Master Mix (Applied Biosystems, Foster City, CA). All data analysis was performed with the $2^{-\Delta\Delta C_t}$ method in Microsoft Excel version 2007. Primer pairs were designed to amplify the 14 exons of the *FLCN* gene (GenBank accession AF517523)(Kunogi et al., 2010) and ~ 8kb of 5'-genomic sequence (Supporting Information Table 1). All primers were evaluated using the National Center for Biotechnology Information BLAST program.

PCR reaction components included 250nM of each primer, 10ng template DNA and SYBR Green Mix in a final volume of 20ul. RQ-PCR conditions were as follows: 10min at 95°C, 40 cycles of 95°C for 15sec and 60°C for 60sec. *Zinc finger protein* gene (*ZNF80* [MIM194553]) and human *serum albumin* gene (*ALB* [MIM103600]) were selected as endogenous controls (Hattori et al., 2006). Genomic DNA from a BHDS patient with a germline missense mutation in the *FLCN* gene was used as a negative control. All samples were run in triplicate. Threshold values were set at 0.8–1.3 for normals, 0.45–0.74 for deletions and 1.6–1.8 for duplication. Experiments were replicated at least twice if a deletion/duplication was suspected.

Multiplex Ligation-Dependent Probe Amplification Assay (MLPA)

Deletion/duplication analysis of the *FLCN* gene was performed by MLPA according to manufacturer's instructions with a commercially available probe mix (P256, *FLCN* probe mix, MRC-Holland, Amsterdam, The Netherlands). In brief, 200ng of genomic DNA in a final volume of 5ul was heated for 5min at 98°C. After cooling to room temperature, 1.5ul of probe mix and 1.5ul SALSA hybridization buffer (MRC-Holland) were added, followed by heat denaturation (1min at 95°C) and hybridization (16h at 60°C). Ligation was performed by adding 32ul of ligation mix at 54°C for 15min, and stopped by incubation for 5min at 98°C. PCR amplification was carried out for 35 cycles in a final volume of 40ul. PCR products were separated by capillary electrophoresis using an ABI 3130XI (Applied Biosystems) with an internal size standard (LIZ 600; Applied Biosystems). Data analysis was performed using GeneMarker v1.6 (SoftGenetics, State College, PA). Threshold values were set at 0.75–1.3 for normals, 0.4–0.65 for deletions and 1.4–1.6 for duplications. Patient data was normalized to data from two deletion-negative controls.

Array-based Comparative Genomic Hybridization (aCGH)

An Agilent Custom High-Definition (HD) (Agilent, Santa Clara, CA) CGH array was designed to investigate the *FLCN* gene copy number using probes from the Agilent HD-CGH database. Seventy-three HD probes within a 25kb genomic region containing the *FLCN* gene were computationally pre-selected with an average probe density of ~3 probes/kb. In the 50kb flanking regions 5' and 3' to *FLCN*, a fade-out design achieved an average density of ~1 probe/kb diminishing to an average of ~1 probe/40kb over the entire genome. The array was printed on an Agilent 4x44K Customer array and processed according to manufacturer's protocol. Briefly, 0.5ug of patient genomic DNA and normal human reference DNA (Promega, Madison, WI) were fragmented by AluI/RsaI digestion, labeled with Cy3/Cy5 fluorescent dyes and hybridized at 65°C for 24hrs. After hybridization and washing, arrays were scanned using Agilent Microarray Scanner. Data were extracted with Agilent Feature Extraction Software (v10.7.1.1) and analyzed with Agilent DNA Analytics 4.0 software (v4.0.85).

Long Range PCR (LR-PCR)

Expand Long Range dNTPack (Roche, Indianapolis, IN) was used according to the manufacturer's instructions using RQ-PCR primers adjacent to deleted regions and additional nested primers (Supporting Information Table 2). DNA fragments were gel purified using DNA Gel Extraction Kit (Qiagen, Valencia, CA).

Sequencing

All purified DNA products were sequenced bidirectionally using the Big Dye Terminator v. 1.1 Cycle Sequencing Kit (Applied Biosystems) according to manufacturer's specifications and run on an ABI 3130xl Genetic Analyzer. RQ-PCR and LR-PCR nested primer pairs were used for sequencing.

FLCN promoter/exon 1 luciferase reporter construction and assay

BAC-cloned human DNA (CTD2 2504A7; Invitrogen, Carlsbad, CA) was double-digested with KpnI and SacI (New England Biolabs, Waltham, MA) to release a fragment containing 4248bp of 5' flanking sequence, *FLCN* exon 1 (228bp) and 673bp of intron 1 that was gel purified using a QIAquick Gel Extraction kit (Qiagen). The fragment was ligated to linearized phosphatase-treated pGL3-Basic vector (Promega) using DNA Ligation Kit (Takara Bio Inc., Madison, WI) according to manufacturer's protocols. The ligation mixture was directly used for transformation into One Shot® Stbl3™ Chemically Competent *E. coli* cells (Invitrogen). Plasmid DNA was extracted using Nucleospin Plasmid kit (Machery-Nagel, Deer Park, NY). The insert (2038bp) of the *FLCN* promoter/exon 1 construct was confirmed as correct by restriction mapping.

To generate the promoter/exon 1 deletion mutant construct, the wild-type *FLCN* promoter/exon 1 construct was digested with SacII (New England Biolabs, Ipswich, MA) to release a 1396bp DNA segment containing 835bp of the CpG island that included all of exon 1. A self-ligation of the resulting ~8.6kb exon 1 deletion construct was performed with the DNA ligation kit (Takara Bio Inc.) and used directly for transformation as above. Plasmid DNA was prepared using Nucleospin Plasmid extraction kit (Macherey-Nagel). The deletion construct was confirmed by restriction mapping as above.

HEK293A cells were transfected with pGL3-Basic empty vector, *FLCN* wild-type and promoter/exon 1 deletion mutant vectors using Lipofectamine 2000 according to the manufacturer's instructions and incubated overnight at 37°C in a CO₂ incubator. Reporter assays using the Dual-Luciferase Reporter 1000 Assay System (Promega) were performed 24hours later according to the manufacturer's instructions. The samples were read in a 96-well plate using MicroLumat^{Plus} LB96V (Berthold Technologies, Oak Ridge, TN). Data analysis was performed in Microsoft Excel version 2007.

RNA extraction, cDNA synthesis and cloning

Patient 11 tumor and normal kidney tissue from a sporadic kidney cancer patient were collected at surgery at the Urologic Oncology Branch, NCI, flash frozen and maintained in liquid N₂ until use. RNA was extracted from tumor tissues using Trizol following homogenization with gentleMACS™ Dissociator (Miltenyi Biotec, Bergisch Gladbach, Germany). cDNA was generated using SuperScript III First-Strand Synthesis SuperMix for qRT-PCR (Invitrogen). To eliminate the contaminating wild-type sequence, the mutant cDNA band from patient 11 tumor RNA was cloned into a TOPO TA cloning vector (Invitrogen) prior to sequencing. A PCR product from patient 11 genomic DNA containing the breakpoint between exon 11 and duplicated exon 10 (exon 10') was cloned into a TOPO TA cloning vector (Invitrogen).

RESULTS

FLCN deletion mapping in BHDS families

DNA from 23 patients in 15 unrelated families with clinically-proven BHDS was analyzed for *FLCN* deletions and duplications. We detected six unique intragenic germline deletions [40% (6/15) of families] by RQ-PCR, which were confirmed by MLPA and aCGH. The results summarized in Table 1 include one deletion spanning exons 2–5, one deletion encompassing exons 7–14, and four deletions that include exon 1.

Patient 1 of Family A had a *FLCN* deletion that spanned exons 2–5, which was identified by RQ-PCR and confirmed by MLPA (Figs. 1A and 1B). LR-PCR was used to amplify the deleted region and produced a ~3kb mutant product compared to the ~12.3kb wild type genomic sequence, predicting a deletion of ~9kb (Fig. 1C). Bidirectional sequencing of the mutant PCR product, confirmed a 9189bp deletion (Fig. 1D; Supporting Information Table 3) that eliminated exons 2–5, including the translation start codon within exon 4, preventing normal translation. The deletion boundaries involving the repeat elements *AluSq* in intron 1 and *AluSx* in intron 5 generated the breakpoint sequence: *AluSq*'-*AluSx*' 5'-GCCATTGCAC-TCCAGCCTGG-3'.

RQ-PCR for patients 2 and 3 in Family B identified a deletion spanning exons 7–14 (Supporting Information Figure 1). By MLPA, a deletion of at least exons 8–14 was detected (Supporting Information Figure 2). The discrepancy in results generated by the RQ-PCR and MLPA methods could be due to differences in the locations of the probes and primers for these two techniques since the MLPA probe for exon 7 is located just 5' of the RQ-PCR primers for this exon. Our methods could not map the extent of this deletion precisely enough for standard long-range PCR amplification to be successful. Other methods such as whole genome sequencing of this region using targeted capture could be applied to fine map the deletion in Family B. Probes designed for aCGH for both patients defined the deletion to include the termination codon (Supporting Information Table 4), but could not clearly determine the status of exon 7, nor the exact extent of the deletion 3' of exon 14.

Four of the six deletions (67%) identified in this study (Families C-F) encompassed exon 1 of *FLCN*. A representative example, Family D (Fig. 2A), is shown in the panels of Fig. 2. Both RQ-PCR (Fig. 2B) and MLPA (Fig. 2C) confirmed a deletion of exon 1 in patients 5 and 6 in Family D, and in Families C, E and F (Supporting Information Figures 1 and 2 and data not shown), but neither method gave information about the deletion boundaries. To determine the 5'-boundary of the deleted sequences in these BHDS families, RQ-PCR with an expanded panel of primers within the ~8kb genomic sequence 5' of exon 1 was utilized. RQ-PCR localized all of the exon 1 deletions in Families C-F to a 4kb region consisting of 5' flanking sequences, exon 1 and a portion of intron 1 (Fig. 3A; Supporting Information Figure 1). Due to the density of aCGH probes in the exon 1 region, we were able to more finely map these deletions using aCGH (Supporting Information Table 4). Primer pairs for LR-PCR were subsequently designed to amplify the mutant fragments in each family. The deletion breakpoints for patient 4 in Family C were identified by bidirectional sequencing of the mutant PCR products (Supporting Information Table 3), and this DNA sample was subsequently used as a positive control for Families D-F. Representative aCGH, LR-PCR, and deletion breakpoint sequencing results for patients 5 and 6 of Family D are shown in Figs. 2D, 2E, and 2F, respectively. Three of the breakpoints identified in the four exon 1 deletion families were characterized using these methods (Table 1). All of the deletions were different, ranging from 5688bp to 6645bp in size, and none included *COPS3*, the gene located approximately 44kb 5' of exon 1 in *FLCN*. Efforts to map the breakpoints of Family F were unsuccessful.

The genomic sequences 5' of exon 1 and within intron 1 have an unusually high number of *Alu* repeat elements identified by RepeatMasker software (38.4%) compared to the rest of the *FLCN* gene (26%) that could be responsible, by homologous recombination, for some of the deletions involving exon 1 (Fig. 3A). The deletions in Families C and E are flanked by *Alu* elements, but the Family D deletion was not flanked by any identifiable repetitive or homologous sequence (Supporting Information Table 3). The mechanism that generated this *FLCN* deletion is therefore unknown. Family E probably underwent a complex, partially *Alu*-mediated rearrangement, resulting in deletion of two sequences, which flanked a short sequence that became inverted. Most probably, an initial inversion event brought a 4006bp sequence and a 2764bp sequence adjacent to one another, permitting a subsequent 6645bp deletion but retaining a 125bp sequence in the reverse orientation (Fig. 3B; Supporting Information Table 3). The *AluY* and *AluSg* elements that flanked the 2764bp sequence may have mediated one, but not both, of these events.

To rule out the possibility that deletions of the non-coding exon 1 sequences were common polymorphisms, MLPA was performed on 52 unrelated patients not affected with BHDS and no exon 1 deletions were found (data not shown). Furthermore, identification of exon 1 deletions in an additional affected family member from each of Families D and E with the same breakpoints as the probands supported their pathogenicity in BHDS.

Identification of *FLCN* promoter region within the exon 1 deletions

Since all of the exon 1 deletions mapped in Families C-E and predicted by aCGH in Family F included additional sequence 5' to exon 1, we speculated that the *FLCN* promoter was also deleted, thereby preventing transcription of the mutant copy of *FLCN*. Bioinformatics resources (UCSC human Genome Browser and Proscan Version 1.7) were used to predict the *FLCN* promoter through identification of CpG islands, open chromatin regions, histone and transcription binding regions. Exon 1 was found to encompass part of the putative promoter. To demonstrate that the common region lost in the exon 1 deletions was functionally important in *FLCN* regulation, we performed luciferase reporter assays. Based on the predictions of the putative promoter region, we designed the wild-type *FLCN* DNA insert for the luciferase reporter vector to include a 5149bp region that contained 4248bp 5' of exon 1, exon 1 (228bp) and 673bp of intron 1. The *FLCN* promoter/exon 1 deletion mutant vector lacked exon 1, a common region deleted in BHDS Families C-F, and retained only ~130bp at the 3' end of the predicted CpG island (Fig. 4A). The mutant vector demonstrated a 31-fold decrease in activity ($p < 0.001$, student t test) when normalized to the activity of the wild type vector (Fig. 4B). These data confirm that the exon 1 deletions found in the germline of BHDS Families C-F are functionally important, and provide the "first hit" leading to loss of *FLCN* tumor suppression and tumorigenesis in BHDS.

FLCN duplication mapping in BHDS Family G

The MLPA results for patients 10 and 11 in BHDS Family G suggested a duplication of exons 10 and 11 (Supporting Information Figure 2), which was confirmed by RQ-PCR (Fig. 5B). cDNA from patient 11 kidney tumor RNA was used to amplify exons 7–12. A 750bp PCR product generated from both patient 11 and control samples corresponded to the wild type cDNA sequence (749bp) (Fig. 5C). An additional ~1kb PCR product, amplified from patient 11 but not the control, was the predicted size (987bp) of the mutant *FLCN* allele containing an exon 10–11 duplication. Sequence analysis demonstrated that exons 10 and 11 were duplicated in tandem in the mature transcript (Supporting Information Table 3; Fig. 5A). The source of a smaller band present in the control but not patient sample was unknown and not analyzed further.

To map the breakpoint between exons 11 and 10' (duplicated exon 10), genomic DNA from patients 10 and 11 was amplified with exon 11 RQ-PCR forward primer and exon 10 RQ-PCR reverse primer producing a mutant product measuring ~750bp that was absent in the control sample (Fig. 5D). This region could not be amplified from wild-type *FLCN* since the primers are facing opposite directions. Bidirectional sequencing of the 778bp fragment using the same PCR primers revealed a sequence containing the 3' end of exon 11, 410bp of the 5'-end of intron 11 joined to 154bp of the 3'-end of intron 9, followed by the 5'-end of exon 10 (Fig. 5E; Supporting Information Table 3). The breakpoint was not flanked by *Alu* repeat elements and only a small percentage of repetitive sequences was found by RepeatMasker in the vicinity of the duplication (11.51% from intron 9 to intron 11, of which 8% were *Alus*).

The exon 10–11 duplication in BHDS Family G (c.1063-154_1300+410dup; p.Glu434GlyfsX35) is predicted to produce a frameshift and premature termination codon. Interestingly, a somatic mutation in the wild-type copy of the *FLCN* gene was identified in the patient 11 kidney tumor that generated a stop codon in exon 12 (data not shown) providing the second “hit” to inactivate the tumor suppressor *FLCN* in the BHD renal tumor.

Genotype-Phenotype correlations

Chart reviews were performed on 9 patients from 6 unrelated families excluding patients 2 and 3, from Family B, for whom phenotypic data were incomplete. The phenotypic data from deletion and duplication patients were pooled to analyze genotype-phenotype correlations and compared to patients with *FLCN* point mutations. Point mutations include small insertions/deletions, nonsense, missense, and splice-site mutations (Toro et al., 2008) (Table 1; Supporting Information Figure 3).

The average age at diagnosis for BHDS for the *FLCN* deletion/duplication families was 47 (range 29–60) compared to 48 (range 31–71) in BHDS patients with point mutations. Age of onset for skin and lung manifestations was not reported (Schmidt et al., 2005). Ninety-one percent (10/11) of patients and 86% (6/7) of families had fibrofolliculomas, excluding patient 4 of Family C who had perifollicular fibromas. Sixty-four percent (7/11) of patients and 71% (5/7) of families had lung cysts. Of those, only patient 9 of Family F developed pneumothoraces (n=3). Twenty-seven percent (3/11) of patients and 29% (2/7) of families had kidney tumors. Among the promoter/exon1 deletion families, only patient 4 of Family C developed bilateral multifocal kidney tumors. Four patients (36%) from four unrelated families (Families A, D, F and G) had thyroid findings including 3 with hypothyroidism, one of whom had become thyroid-dependent following a total thyroidectomy and radiation for papillary thyroid cancer. Patient 5 of Family D had a benign thyroid nodule. With the exception of the thyroid findings, the frequency of symptoms reported in patients with *FLCN* deletions/duplications, or point mutations was similar (Supporting Information Figure 3).

DISCUSSION

We have identified six intragenic deletions and one duplication in 47% (7/15) of unrelated BHDS families and characterized 5 of 7 breakpoints. Our data confirm that, in addition to protein-altering *FLCN* frameshift, missense, nonsense and splice-site mutations, BHDS can be caused by large intragenic deletions as first described by Kunogi et al. (Kunogi et al., 2010). Significantly, we have identified a “hot spot” in the exon 1/promoter region for *FLCN* deletions and present here the first reported case of a large intragenic *FLCN* duplication.

Alu repeats are associated with and may explain the majority of *FLCN* deletions characterized in our cohort. Sixty percent (3/5) of the deletions identified (Families A, C and

E) were flanked by *Alu* repeats (SINEs), reported to be involved in Non-Allelic Homologous Recombination (NAHR) (Deininger et al., 1999) in *Alu*-mediated deletions implicated in other human cancers including VHL, breast cancer, Ewing's sarcoma and HNPCC (Lehrman et al., 1986; Mauillon et al., 1996).

The *FLCN* intragenic deletions in Families E and D involved more complex structural rearrangements. The inversion and subsequent intragenic deletion in Family E was the result of a recombination involving *AluSg*- and *AluY*-flanked sequences, and another recombination event of unknown mechanism. The Family E deletion retained *AluY* sequences at the 5'-deletion boundary but no definable repetitive elements at the 3'-deletion boundary; an *AluJb* is located 982bp away. A similar mechanism has been described for the bleeding disorder Glanzmann Thrombasthenia (GT), where an *Alu*-mediated inversion occurred followed by an *Alu*-mediated deletion (Li et al., 1993). The intragenic *FLCN* deletion in Family D had no repetitive elements or homology to another DNA sequence on either side of the deletion boundaries. The closest repetitive elements were *THE1B* located 436bp from the 5'-boundary, and *AluJ*, located 1106bp from the 3'-deletion boundary. As has been suggested, (Stankiewicz et al., 2003; Lee et al., 2006) it is possible that repetitive elements near the gene could facilitate the deletion.

Low copy repeats (LCR) are DNA elements ranging from 1–200kb in size with >90% homology, which have been implicated in many chromosome 17 genetic rearrangements (Shchelochkov et al., 2010). The density of these elements in the human genome ranges from 5–10%. However, their frequency in the proximal region of chromosome 17 is 23%, possibly accounting for the high rate of genetic rearrangements (Shchelochkov et al., 2010). Stankiewicz et al. investigated the breakpoints of 18 genetic rearrangements in chromosome 17 and identified 9 patients (50% of their cohort) with LCRs at one breakpoint and non-LCR DNA sequences at the other boundary as identified in Family E (Stankiewicz et al., 2003). Inoue et al. (2002) also described 2 Pelizaeus-Merzbacher (*PLP1*) families with deletions but no identifiable homologous sequences at the breakpoint boundaries. Possible mechanisms for the generation of these deletions include NAHR using only small segments of homology or Non-Homologous DNA End-Joining (NHEJ) where no homology is necessary (Lieber et al., 2003). Another possibility is that novel repetitive elements could be involved in these rearrangements. These systems may not be mutually exclusive of each other.

We have identified the first intragenic duplication in the *FLCN* gene. Although *Alu*-mediated intragenic duplications have been well-described, (Schichman et al., 1994; Yap et al., 2006) no *Alu* repeats or other repetitive elements were found at the breakpoint junction in BHDS Family G. We speculate that nonhomologous recombination or small homologous mechanisms are involved in the generation of the tandem duplication. Several examples in the literature, including two Duchenne muscular dystrophy families (Hu et al., 1991) and a split hand-split foot malformation 3 (SHFM3) family (de Mollerat et al., 2003) in which duplication events occurred at breakpoints without homologous sequences, further demonstrate that nonhomologous duplication events occur, although the mechanism remains poorly understood.

Our results demonstrate the importance of utilizing RQ-PCR, MLPA and/or aCGH as diagnostic methods in BHDS patients who are *FLCN* mutation-negative by DNA sequencing, especially for the *FLCN* promoter/exon1 region, where 67% of the deletions identified were located, and no point mutations had been reported (Toro et al., 2008; Schmidt et al., 2005). However, deletions and duplications involving exons did not account for all cases of BHDS in patients who were mutation-negative by sequencing (8/15 families, 53% of this cohort). Our RQ-PCR method will detect deletions and duplications within

exonic regions of *FLCN*, but will miss smaller deletions, duplications and other genetic rearrangements within introns (especially large introns 1, 3, 8 and 9) as well as epigenetic alterations and variations in the distal end of the 3'UTR.

The deletions and duplication we characterized most likely affect either the amount or function of the FLCN protein. Based on the marginal activity of the exon1/promoter deletion in the luciferase reporter assay, the exon 1 deletions in BHDS Families C-F would be predicted to dramatically reduce *FLCN* expression from the mutant allele suggesting that the commonly deleted region in these exon 1 deletion families contains the *FLCN* minimal promoter region.

The exon 2–5 deletion in BHDS Family A includes the initiation codon in exon 4, preventing normal translation. The duplication of exons 10 and 11 in BHDS Family G alters the reading frame of the transcribed mRNA resulting in a premature termination codon. The exon 7–14 deletion in BHDS Family B removes much of the coding region and the termination codon. If any protein were made from the encoded mRNA, its function would most likely be disrupted since FNIP1 and FNIP2, the FLCN-interacting proteins that also interact with AMPK, bind to the C-terminus of the FLCN protein (Baba et al., 2006; Hasumi et al., 2008; Takagi et al., 2008). However, in most cases, the generation of a premature termination codon would result in degradation of the *FLCN* mRNA by nonsense mediated decay (NMD) (Chang et al., 2007).

Phenotypic findings in the BHDS patients with *FLCN* deletions or duplication are very similar to those in the point mutation-positive patients (Schmidt et al., 2005). Although major conclusions cannot be drawn from the small number of deletion and duplication-positive families (n=7), a few observations can be made. The most prominent findings are fibrofolliculomas, followed by lung cysts and kidney neoplasms. One patient had perifollicular fibromas (PFF), which have been described as part of the BHDS phenotype (Toro et al., 2008). Notably, only one of 6 patients in the deletion-positive families developed kidney tumors. No significant difference was noted in the frequency of observed/ reported phenotypic features between point mutation-positive patients and patients with a deletion or duplication. Additionally we report 6 of 15 patients with thyroid findings. A few BHDS cases have been described with thyroid adenomas or multinodular goiter, (De La Torre et al., 1999; Drummond et al., 2002) but the question of whether *FLCN* plays a role in thyroid pathology, or BHD-associated thyroid findings reflect the high prevalence of thyroid disease in the general population (Rallison et al., 1991), will await larger studies.

In conclusion this study confirms that large intragenic deletions in *FLCN*, in addition to sequence-altering germline mutations, are causative for BHDS, and reports the first large *FLCN* duplication in a BHDS patient. Large intragenic deletions and duplications of *FLCN* may account for at least 5% of cases of BHDS. Consequently RQ-PCR, MLPA and/or aCGH should be employed for clinical molecular diagnosis of BHDS in patients who are *FLCN* mutation-negative by DNA sequencing.

Supplementary Material

Refer to Web version on PubMed Central for supplementary material.

Acknowledgments

We thank the National Institutes of Health Undergraduate Scholarship Program for their funding, James Peterson and Lindsay Middleton for providing pedigree and phenotypic data, and Dr. Makiko Kunogi for helpful discussions regarding RQ-PCR. This research was supported in part by the Intramural Research Program of the National Institute of Health, National Cancer Institute, Center for Cancer Research and funded in part with federal funds

from the National Cancer Institute, National Institutes of Health, under contract HHSN261200800001E. The content of this publication does not necessarily reflect the views or policies of the Department of Health and Human Services, nor does mention of trade names, commercial products, or organizations imply endorsement by the U.S. Government.

References

- Ahvenainen T, Lehtonen HJ, Lehtonen R, Vahteristo P, Aittomaki K, Baynam G, Dommering C, Eng C, Gruber SB, Gronberg H, Harvima R, Herva R, Hietala M, Kujala M, Kaariainen H, Sunde L, Vierimaa O, Pollard PJ, Tomlinson IP, Bjorck E, Aaltonen LA, Launonen V. Mutation screening of fumarate hydratase by multiplex ligation-dependent probe amplification: detection of exonic deletion in a patient with leiomyomatosis and renal cell cancer. *Cancer Genet Cytogenet.* 2008; 183:83–88. [PubMed: 18503824]
- Baba M, Hong SB, Sharma N, Warren MB, Nickerson ML, Iwamatsu A, Esposito D, Gillette WK, Hopkins RF III, Hartley JL, Furihata M, Oishi S, Zhen W, Burke TR Jr, Linehan WM, Schmidt LS, Zbar B. Folliculin encoded by the BHD gene interacts with a binding protein, FNIP1, and AMPK, and is involved in AMPK and mTOR signaling. *Proc Natl Acad Sci U S A.* 2006; 103:15552–15557. [PubMed: 17028174]
- Birt AR, Hogg GR, Dube WJ. Hereditary multiple fibrofolliculomas with trichodiscomas and acrochordons. *Arch Dermatol.* 1977; 113:1674–1677. [PubMed: 596896]
- Chang YF, Imam JS, Wilkinson MF. The nonsense-mediated decay RNA surveillance pathway. *Annu Rev Biochem.* 2007; 76:51–74. [PubMed: 17352659]
- De La Torre C, Ocampo C, Doval IG, Losada A, Cruces MJ. Acrochordons are not a component of the Birt-Hogg-Dube syndrome: does this syndrome exist? Case reports and review of the literature. *Am J Dermatopathol.* 1999; 21:369–374. [PubMed: 10446780]
- De Mollerat XJ, Gurrieri F, Morgan CT, Sangiorgi E, Everman DB, Gaspari P, Amiel J, Bamshad MJ, Lyle R, Blouin JL, Allanson JE, Le Marec B, Wilson M, Braverman NE, Radhakrishna U, Delozier-Blanchet C, Abbott A, Elghouzzi V, Antonarakis S, Stevenson RE, Munnich A, Neri G, Schwartz CE. A genomic rearrangement resulting in a tandem duplication is associated with split hand-split foot malformation 3 (SHFM3) at 10q24. *Hum Mol Genet.* 2003; 12:1959–1971. 35. [PubMed: 12913067]
- Deininger PL, Batzer MA. Alu repeats and human disease. *Mol Genet Metab.* 1999; 67:183–193. [PubMed: 10381326]
- Drummond C, Grigoris I, Dutta B. Birt-Hogg-Dube syndrome and multinodular goitre. *Australas J Dermatol.* 2002; 43:301–304. [PubMed: 12423440]
- Franke G, Bausch B, Hoffmann MM, Cybulla M, Wilhelm C, Kohlhase J, Scherer G, Neumann HP. Alu-Alu recombination underlies the vast majority of large VHL germline deletions: Molecular characterization and genotype-phenotype correlations in VHL patients. *Hum Mutat.* 2009; 30:776–786. [PubMed: 19280651]
- Hasumi H, Baba M, Hong SB, Hasumi Y, Huang Y, Yao M, Valera VA, Linehan WM, Schmidt LS. Identification and characterization of a novel folliculin-interacting protein FNIP2. *Gene.* 2008; 415:60–67. [PubMed: 18403135]
- Hasumi Y, Baba M, Ajima R, Hasumi H, Valera V, Klein M, Haines D, Merino M, Hong SB, Yamaguchi T, Schmidt LS, Linehan WM. Homozygous loss of BHD causes early embryonic lethality and kidney tumor development with activation of mTORC1 and mTORC2. *Proc Natl Acad Sci USA.* 2009; 106:18722–18727. [PubMed: 19850877]
- Hattori K, Teranishi J, Stolle C, Yoshida M, Kondo K, Kishida T, Kanno H, Baba M, Kubota Y, Yao M. Detection of germline deletions using real-time quantitative polymerase chain reaction in Japanese patients with von Hippel-Lindau disease. *Cancer Sci.* 2006; 97:400–405. [PubMed: 16630138]
- Hoebeek J, van der Luijt R, Poppe B, De SE, Yigit N, Claes K, Zewald R, de Jong GJ, De PA, Speleman F, Vandesompele J. Rapid detection of VHL exon deletions using real-time quantitative PCR. *Lab Invest.* 2005; 85:24–33. [PubMed: 15608663]

- Hu XY, Ray P, Worton RG. Mechanisms of tandem duplication in the Duchenne muscular dystrophy gene include both homologous and nonhomologous intrachromosomal recombination. *EMBO J*. 1991; 10:2471–2477. [PubMed: 1868831]
- Inoue K, Osaka H, Thurston VC, Clarke JT, Yoneyama A, Rosenbarker L, Bird TD, Hodes ME, Shaffer LG, Lupski JR. Genomic rearrangements resulting in PLP1 deletion occur by nonhomologous end joining and cause different dysmyelinating phenotypes in males and females. *Am J Hum Genet*. 2002; 71:838–853. [PubMed: 12297985]
- Kunogi M, Kurihara M, Ikegami TS, Kobayashi T, Shindo N, Kumasaka T, Gunji Y, Kikkawa M, Iwakami S, Hino O, Takahashi K, Seyama K. Clinical and genetic spectrum of Birt-Hogg-Dubé Syndrome patients in whom pneumothorax and/or multiple lung cysts are the presenting feature. *J Med Genet*. 2010; 47:281–287. [PubMed: 20413710]
- Lee JA, Madrid RE, Sperle K, Ritterson CM, Hobson GM, Garbern J, Lupski JR, Inoue K. Spastic paraplegia type 2 associated with axonal neuropathy and apparent PLP1 position effect. *Ann Neurol*. 2006; 59:398–403. [PubMed: 16374829]
- Lehrman MA, Russell DW, Goldstein JL, Brown MS. Exon-Alu recombination deletes 5 kilobases from the low density lipoprotein receptor gene, producing a null phenotype in familial hypercholesterolemia. *Proc Natl Acad Sci U S A*. 1986; 83:3679–3683. [PubMed: 3012527]
- Li L, Bray PF. Homologous recombination among three intragene Alu sequences causes an inversion-deletion resulting in the hereditary bleeding disorder Glanzmann thrombasthenia. *Am J Hum Genet*. 1993; 53:140–149. [PubMed: 8317479]
- Lieber MR, Ma Y, Pannicke U, Schwarz K. Mechanism and regulation of human non-homologous DNA end-joining. *Nat Rev Mol Cell Biol*. 2003; 4:712–720. [PubMed: 14506474]
- Mauillon JL, Michel P, Limacher JM, Latouche JB, Dechelotte P, Charbonnier F, Martin C, Moreau V, Metayer J, Paillot B, Frebourg T. Identification of novel germline hMLH1 mutations including a 22 kb Alu-mediated deletion in patients with familial colorectal cancer. *Cancer Res*. 1996; 56:5728–5733. [PubMed: 8971183]
- McWhinney SR, Pilarski RT, Forrester SR, Schneider MC, Sarquis MM, Dias EP, Eng C. Large germline deletions of mitochondrial complex II subunits SDHB and SDHD in hereditary paraganglioma. *J Clin Endocrinol Metab*. 2004; 89:5694–5699. [PubMed: 15531530]
- Nickerson ML, Warren MB, Toro JR, Matrosova V, Glenn G, Turner ML, Duray P, Merino M, Choyke P, Pavlovich CP, Sharma N, Walther M, Munroe D, Hill R, Maher E, Greenberg C, Lerman MI, Linehan WM, Zbar B, Schmidt LS. Mutations in a novel gene lead to kidney tumors, lung wall defects, and benign tumors of the hair follicle in patients with the Birt-Hogg-Dubé Syndrome. *Cancer Cell*. 2002; 2:157–164. [PubMed: 12204536]
- Rallison ML, Dobyns BM, Meikle AW, Bishop M, Lyon JL, Stevens W. Natural history of thyroid abnormalities: prevalence, incidence, and regression of thyroid diseases in adolescents and young adults. *Am J Med*. 1991; 91:363–370. [PubMed: 1951380]
- Schichman SA, Caligiuri MA, Gu Y, Strout MP, Canaani E, Bloomfield CD, Croce CM. ALL-1 partial duplication in acute leukemia. *Proc Natl Acad Sci U S A*. 1994; 91:6236–6239. [PubMed: 8016145]
- Schmidt LS, Warren MB, Nickerson ML, Weirich G, Matrosova V, Toro JR, Turner ML, Duray P, Merino M, Hewitt S, Pavlovich CP, Glenn G, Greenberg CR, Linehan WM, Zbar B. Birt-Hogg-Dubé syndrome, a genodermatosis associated with spontaneous pneumothorax and kidney neoplasia, maps to chromosome 17p11.2. *Am J Hum Genet*. 2001; 69:876–882. [PubMed: 11533913]
- Schmidt LS, Nickerson ML, Warren MB, Glenn GM, Toro JR, Merino MJ, Turner ML, Choyke PL, Sharma N, Peterson J, Morrison P, Maher ER, Walther MM, Zbar B, Linehan WM. Germline BHD-mutation spectrum and phenotype analysis of a large cohort of families with Birt-Hogg-Dubé syndrome. *Am J Hum Genet*. 2005; 76:1023–1033. [PubMed: 15852235]
- Shchelochkov OA, Cheung SW, Lupski JR. Genomic and clinical characteristics of microduplications in chromosome 17. *Am J Med Genet*. 2010; 152A:1101–1110. [PubMed: 20425816]
- Stankiewicz P, Shaw CJ, Dapper JD, Wakui K, Shaffer LG, Withers M, Elizondo L, Park SS, Lupski JR. Genome architecture catalyzes nonrecurrent chromosomal rearrangements. *Am J Hum Genet*. 2003; 72:1101–1116. [PubMed: 12649807]

- Swensen J, Hoffman M, Skolnick MH, Neuhausen SL. Identification of a 14 kb deletion involving the promoter region of BRCA1 in a breast cancer family. *Hum Mol Genet.* 1997; 6:1513–1517. [PubMed: 9285788]
- Takagi Y, Yobayashi T, Shiono M, Wang L, Piao X, Sun G, Zhang D, Abe M, Hagiwara W, Takahashi K. Interaction of folliculin (Birt-Hogg-Dubé gene product) with a novel Fnip1-like (Fnip1/Fnip2) protein. *Oncogene.* 2008; 27:5339–5347. [PubMed: 18663353]
- Toro JR, Glenn G, Duray P, Darling T, Weirich G, Zbar B, Linehan WM, Turner ML. Birt-Hogg-Dube syndrome: a novel marker of kidney neoplasia. *Arch Dermatol.* 1999; 135:1195–1202. [PubMed: 10522666]
- Toro JR, Wei M-H, Glenn GM, Weinreich M, Tour O, Vocke C, Turner M, Choyke P, Merino MJ, Pinto PA, Steinberg SM, Schmidt LS, Linehan WM. BHD mutations, clinical and molecular genetic investigations of Birt-Hogg-Dube syndrome: a new series of 50 families and a review of published reports. *J Med Genet.* 2008; 45:321–331. [PubMed: 18234728]
- Vocke CD, Yang Y, Pavlovich CP, Schmidt LS, Nickerson ML, Torres-Cabala CA, Merino MJ, Walther MM, Zbar B, Linehan WM. High frequency of somatic frameshift BHD gene mutations in Birt-Hogg-Dube-associated renal tumors. *J Natl Cancer Inst.* 2005; 97:931–935. [PubMed: 15956655]
- Warren MB, Torres-Cabala CA, Turner ML, Merino MJ, Matrosova VY, Nickerson ML, Ma W, Linehan WM, Zbar B, Schmidt LS. Expression of Birt-Hogg-Dube gene mRNA in normal and neoplastic human tissues. *Mod Pathol.* 2004; 17:998–1011. [PubMed: 15143337]
- Yap KP, Ang P, Lim IH, Ho GH, Lee AS. Detection of a novel Alu-mediated BRCA1 exon 13 duplication in Chinese breast cancer patients and implications for genetic testing. *Clin Genet.* 2006; 70:80–82. [PubMed: 16813611]

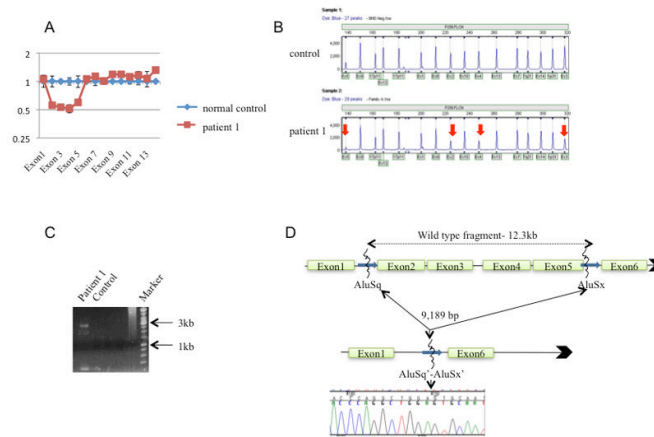


Figure 1. Mapping of *FLCN* exon 2–5 deletion in patient 1 of BHDS Family A.

A. RQ-PCR of genomic DNA from patient 1 demonstrated a heterozygous deletion of exons 2–5. B. MLPA analysis revealed a heterozygous deletion of exons 2–5 of the *FLCN* gene in patient 1 (lower panel) compared with normal control (upper panel). C. LR-PCR of patient 1 DNA generated a smaller mutant fragment of ~3kb not seen in control sample. D. Sequencing of the breakpoint confirmed a deletion of 9189bp. The breakpoint contained sequences from both *AluSq* and *AluSx* repeat elements at the 5'- and 3'-boundaries of the deletion.

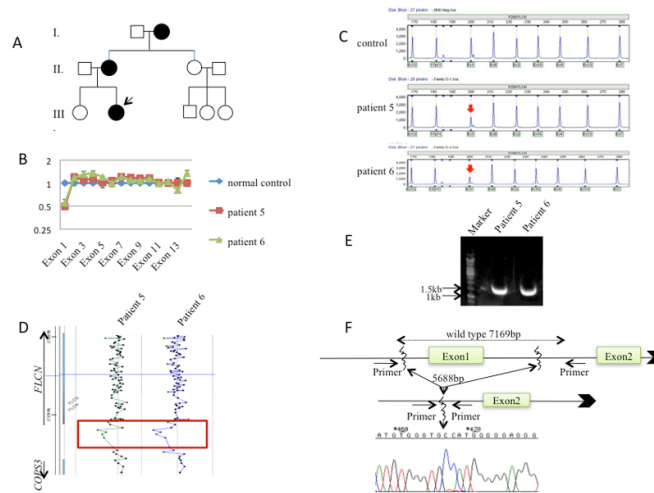


Figure 2. Mapping of *FLCN* exon 1 deletions in patients 5 and 6 of BHDS Family D

A. Pedigree of Family D. Arrow indicates proband (patient 6). B. RQ-PCR of DNA from patients 5 (mother) and 6 (proband) demonstrated a heterozygous deletion of exon 1 of the *FLCN* gene. C. MLPA analysis revealed a heterozygous deletion of exon 1 for patients 5 and 6 (lower panels) compared with normal control (upper panel). D. aCGH results for patients 5 and 6. Red box, deleted region including exon 1. E. LR-PCR of region of interest in DNA from patients 5 and 6 yielded smaller mutant products of ~1.5kb using primers BHDpromoter4 and BHDintron1d. F. Sequencing of mutant PCR products confirmed deletion of 5688bp in both proband and mother, which is not flanked by *Alu* repeat elements. Large arrowhead indicates 5'-3' direction.

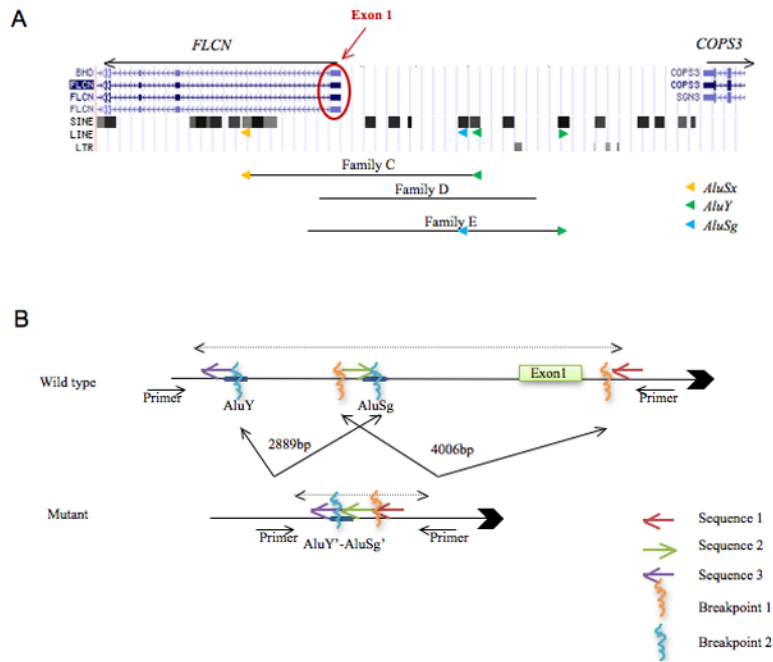


Figure 3. Genomic location of *FLCN* exon 1 deletions in BHDS Families C, D and E and map of complex *FLCN* deletion in BHDS Family E

A. Location of all mapped exon 1 deletions relative to location of known SINE, LINE and LTR repeat elements. The black lines represent the deleted segments in Families C, D and E. All mapped deletions are unique and none involves the adjacent upstream gene, *COPS3*. Colored triangles, *Alu* sequences.

B. The complex *FLCN* deletion in Family E most likely resulted from an initial inversion event that involved an exon 1-containing 4006bp sequence flanked by breakpoint 1 boundaries (orange vertical lines), or a 2889bp sequence upstream of exon 1 flanked by breakpoint 2 boundaries containing *Alu* sequences (blue vertical lines). A subsequent 6645bp deletion event occurred that eliminated exon 1 but retained a 125bp sequence (green arrow) in the reverse orientation. The *AluY* and *AluSg* elements that flanked the 2889bp sequence may have mediated one, but not both, of these events. Red arrow, intron 1 sequence; purple arrow, sequence 5' to deleted sequences. Large arrowhead indicates 5'-3' direction.

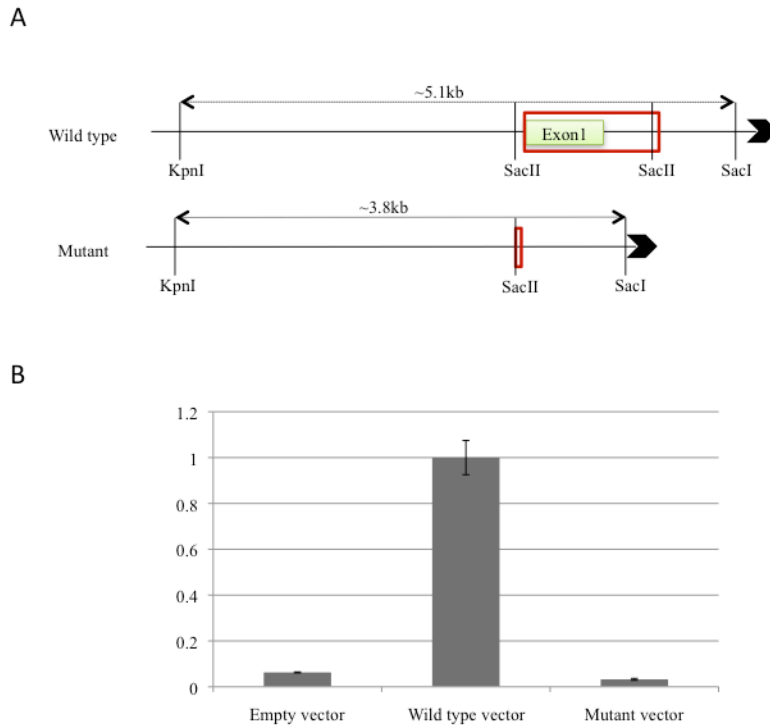


Figure 4. *FLCN* promoter/exon 1 luciferase reporter assay

A. A wild type *FLCN* promoter/exon 1 DNA fragment containing a 5149bp region encompassing 4248bp 5' of exon 1, exon 1 (228bp) and 673bp of intron 1 was inserted into the pGL3 luciferase reporter vector. A mutant *FLCN* promoter/exon 1 deletion fragment that lacked exon 1, a region commonly deleted in BHDS Families C, D, E, and F, was inserted into the luciferase reporter vector. B. *FLCN* promoter/exon 1 deletion mutant vector displayed 31 fold less activity than the wild-type *FLCN* luciferase reporter vector when transfected into HEK293-A cells. Empty vector control is included for comparison. Y-axis, relative activity normalized to wild-type *FLCN* luciferase reporter activity. Red box, predicted CpG island sequence. Large arrowhead indicates 5'-3' direction.

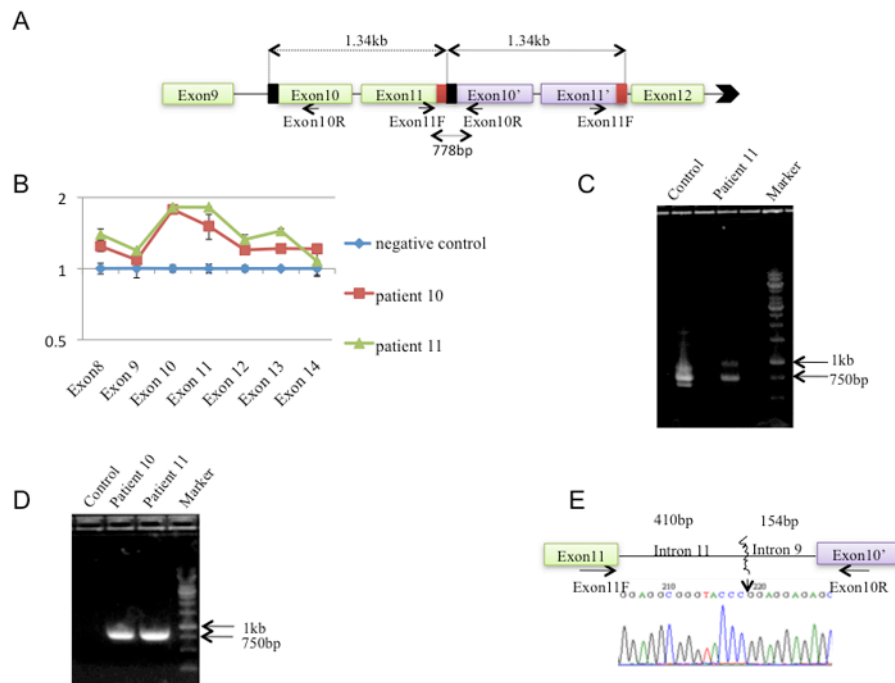


Figure 5. Mapping of *FLCN* exons 10 and 11 duplication identified in BHDS Family G
 A. Schematic diagram showing the 1.34kb duplication of exons 10 and 11 of the *FLCN* gene in tandem with wild-type exons 10 and 11. PCR amplification of patient 11 DNA using exon11QF and exon10QR primers produced a 778bp product that included intron 9 sequence (black box) and intron 11 sequence (red box). B. RQ-PCR of DNA from patients 10 and 11 revealed a heterozygous duplication of exons 10 and 11. C. PCR amplification of *FLCN* cDNA from patient 11 tumor samples revealed both wild-type and larger mutant products resulting from the duplication event. D. PCR amplification of the exons 11 and 10' breakpoint in genomic sequence of proband and his affected sister. E. Sequencing of mutant *FLCN* duplication PCR product defined the breakpoint.

Table 1

Summary of germline *FLCN* deletions/duplication and BHDS family phenotype

Patient	Family	<i>FLCN</i> region	Deletion/Duplication Nucleotide (protein)	Size (bp)	Phenotype
1	A	Exons 2–5	c.-227-853_c.397-295del	9189	FF, 2 LC, hypothyroidism
2	B	Exons 7–14	c.675-?_c.*+?del	ND	FF
3	B	Exons 7–14	c.675-?_c.*+?del	ND	FF
4	C	Exon 1	chr17:17078506_17084897del	6391	PFF, BMF kidney (chromophobe)
5	D	Exon 1	chr17:17080610_17086298del; insCCATGGGGG	5688	FF, LC, benign solitary thyroid nodule
6	D	Exon 1	chr17:17080610_17086298del; insCCATGGGGG	5688	FF, LC
7	E	Exon 1	chr17:17080497_17087267del; 17084378_17084502invins	6645	FF, LC
8	E	Exon 1	chr17:17080497_17087267del; 17084378_17084502invins	6645	FF, LC
9	F	Exon 1	ND	ND	FF, LC, 3PT, hypothyroidism
10	G	Exons 10–11	c.1063-154_1300+410dup (p.Glu434GlyfsX35)	1341	FF, BMF kidney (chromophobe)
11	G	Exons 10–11	c.1063-154_1300+410dup (p.Glu434GlyfsX35)	1341	FF, LC, BMF kidney, papillary thyroid cancer

ND=not determined;

* termination codon; FF= fibrofolliculomas; LC= lung cysts; PFF= perifollicular fibroma; BMF= bilateral multifocal; PT=pneumothorax. For families A, B and G, GenBank Accession: NM_144997.5. For families C, D, and E, coordinates are based on the March 2006 human reference sequence (NCBI Build 36.1/hg18). Family F was not mapped.